Synthesis, Characterization and Antiproliferative Activity of Transition Metal Complexes with 3-(4,5-Diphenyl-1,3-oxazol-2-yl)propanoic Acid (Oxaprozin)

Bojan DJ Božić,[a] Jelena R Rogan,[a] Dejan D Poleti,[a] Nemanja P Trišović,[a] Biljana DJ Božić,[b] and Gordana S Ušćumlić*,[a]

[a] *Faculty of Technology and Metallurgy, University of Belgrade; Karnegijeva 4, 11000 Belgrade, Serbia: and* [b] *Faculty of Biology, University of Belgrade; Studentski trg 3, 11000 Belgrade, Serbia.*
Received February 22, 2012; accepted April 12, 2012

A series of novel Mn(II), Co(II), Ni(II), Cu(II) and Zn(II) complexes with oxaprozin (Hoxa), a non-steroidal anti-inflammatory drug, has been synthesized. The drug and complexes have been characterized by elemental and thermogravimetric (TG) analysis, Fourier transform (FT)-IR, ^{1}H-NMR, ^{13}C-NMR, UV-Vis spectroscopy and magnetic susceptibility measurements. The (pseudo)octahedral geometry has been proposed for all complexes based on electronic spectra and magnetic moments. With exception of the Cu(II) complex, where bridging bidentate mode of COO groups has been found, FT-IR spectra confirmed chelately coordinated COO groups in the other complexes. The general formula of the complexes is $[M(H_2O)_2(oxa)_2]\cdot xH_2O$, with $x=2$ for M=Mn, Co and Ni and $x=1.5$ for Zn. The binuclear Cu(II) complex, $[Cu_2(H_2O)_2(OH)(oxa)_3]\cdot 2H_2O$, has strong Cu–Cu interactions of antiferromagnetic type. The complexes and Hoxa did not exhibit the cytotoxic effect to peritoneal macrophages. For the first time these complexes have been tested for their *in vitro* antiproliferative activity against human colon and breast cancer cell lines, HCT-116 and MDA-231, respectively. For all investigated compounds significant antiproliferative effects have been observed. Ni(II) complex has been shown to be a promising antiproliferative agent exerting excellent activity against HCT-116 even in nanomolar concentrations.

Key words oxaprozin; transition metal complex; antiferromagnetic interaction; cytotoxic effect; antiproliferative activity

Oxaprozin (3-(4,5-diphenyl-1,3-oxazol-2-yl)propanoic acid), Hoxa, belongs to the class of non-steroidal anti-inflammatory drugs (NSAIDs) with analgesic and antipyretic properties.[1)] Its therapeutic effects result from a selective inhibition of the enzyme cyclooxygenase-2 (COX-2), which is largely responsible for the production of prostaglandins in most pathological states.[2)] Epidemiological studies have indicated that continuous therapy with NSAIDs make real promise of chemoprevention and adjunct therapy for cancer patients.[3,4)] It has been demonstrated that COX-2 overexpression is involved in the invasion and growth of cancer,[5)] and blockade of COX-2 function by corresponding drugs can reduce cancer progression in experimental models.[6,7)] On the other hand, beneficial effects of NSAIDs can be additionally explained by an independent mechanism of action in relation to the COX-inhibition pathway.[8)] COX-independent effects of NSAIDs are mediated through modulation of activity of various intracellular kinases, *e.g.* extracellular signal-regulated kinase (ERK), AkT, p38 mitogen activated protein kinase (MAPK), c-Jun N-terminal kinase (JNK),[9–12)] which can lead to the change in activity and expression of some transcription factors (*e.g.* nuclear factor (NF)-κB, Erg-1, AP-1, p-53, PPARγ) inducing apoptosis.[13–16)]

The first row transition metal (TM) ions have attracted significant attention, because they represent trace element that occurs in the reactive centers of many enzymes.[17–21)] It has been demonstrated that TM complexes of NSAIDs are more active than their parent drugs and exhibit lower side-effects.[22)] Thus, some TM complexes with naproxen [(+)-(*S*)-2-(6-methoxynaphthalen-2-yl)propanoic acid], express significant anti-inflammatory effect.[23)] A square planar Cu(II) complex with ketoprofen [(*R*,*S*)-2-(3-benzoylphenyl)propanoic acid] has exhibited enhanced antiproliferative effects on human breast cancer cell line T47D rich in progesterone receptors.[24)] The radical scavenging activity of Hoxa is synergistically enhanced upon Cu(II) coordination in $[Cu_2(DMSO)_2(oxa)_4]$.[25)] All this facts indicate that TM complexes with oxa^- ligand might exhibit additional biological activities and encouraged us to carry out a study of their antiproliferative activity.

In this study, five new oxa TM complexes containing Mn(II), Co(II), Ni(II), Cu(II) and Zn(II) ions were synthesized and characterized. The complexes, as well as Hoxa were also tested *in vitro* against human colon and breast cancer cell lines, HCT-116 and MDA-231, respectively, by 3-(4,5-dimethylthiazol-2-yl)-2,5-diphenyltetrazolium bromide (MTT) assay.

Experimental

General Procedure The starting materials were obtained from Aldrich and Fluka, and were used without further purification.

All the investigated compounds were synthesized following the procedure presented in the synthetic scheme (Chart 1). In detail, oxaprozin, Hoxa, (2.0 mmol) was added to the aqueous solution containing 2.0 mmol of NaOH in 50 mL H_2O. This solution was continuously stirred at 40°C for 2 h, while a clear solution of Naoxa was formed. Then a solution of Naoxa was added dropwise at room temperature in aqueous $M(NO_3)_2$ solution (9.0 mL of 0.1 M; 0.9 mmol), M=Mn(II), Co(II), Ni(II), Cu(II) and Zn(II), under violent stirring for 1 h. Immediately formed precipitate was filtered off after standing overnight, washed several times with distilled water and absolute ethanol and dried in a vacuum at room temperature.

The elemental analysis of the Hoxa and its complexes were

The authors declare no conflict of interest.

* To whom correspondence should be addressed. e-mail: goca@tmf.bg.ac.rs

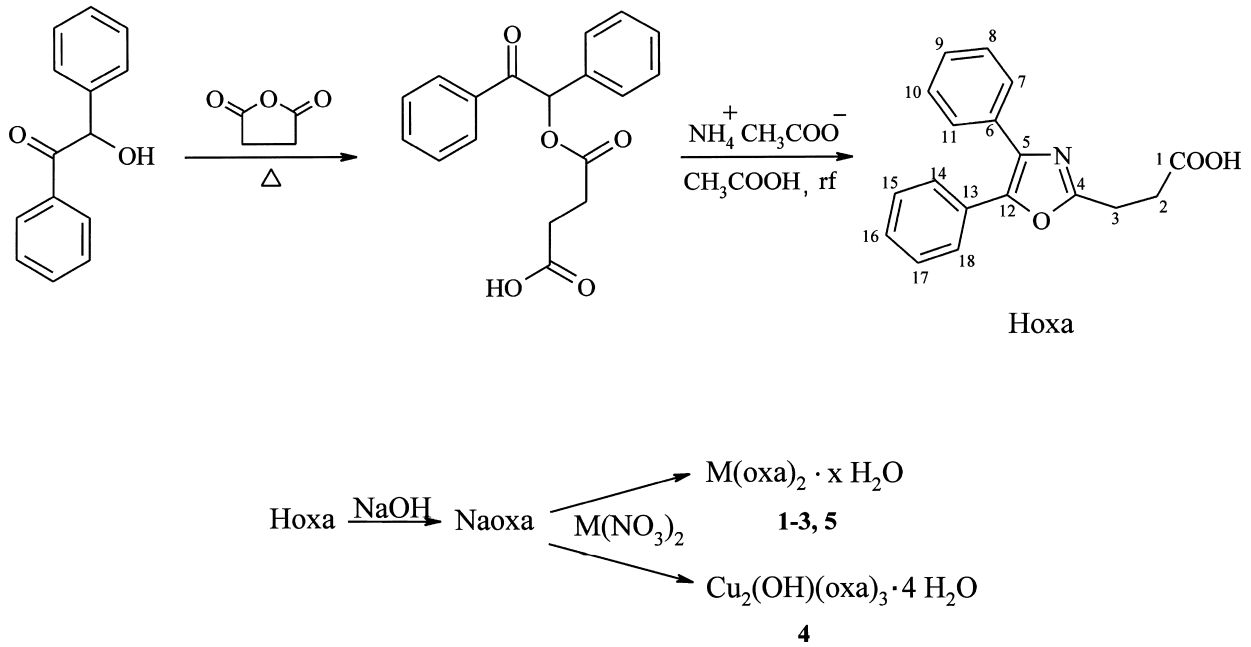

Chart 1. Synthesis of Hoxa and TM Complexes, Where M=Mn (**1**), Co (**2**), Ni (**3**), Cu (**4**), Zn (**5**); x=4 for **1**–**3**, x=3.5 for **5**)

carried out by standard analytical micromethods using an Elemental Vario EL III microanalyzer. Total content of water of crystallization was determined by thermogravimetric (TG) analysis performed from room temperature up to 300°C on an SDT Q600 TGA/DSC instrument (TA Instruments) with heating rate of 20°C min^{-1} in a dry nitrogen atmosphere (flow rate of 100 cm^3 min^{-1}). The ^{1}H- and ^{13}C-NMR spectral measurement of Hoxa was performed on a Bruker AC 250 spectrometer at 200 MHz for ^{1}H-NMR and 50 MHz for ^{13}C-NMR spectra. The spectrum was recorded at room temperature in DMSO-d_6. The chemical shifts are expressed in ppm values referenced to TMS (δ_H=0 ppm) in ^{1}H-NMR spectra, and the residual solvent signal (δ_C=39.5 ppm) in ^{13}C-NMR spectra. FT-IR spectra in the 4000–400 cm^{-1} range were recorded on a Bomem MB 100 FT-IR spectrophotometer in the form of KBr pellets. The electronic spectra of the complexes were recorded by solution techniques using dimethyl sulfoxide (DMSO) as a solvent with Shimadzu 1700 spectrophotometer. Magnetic susceptibility measurements were made at room temperature using an MSB-MK1 magnetic susceptibility balance (Sherwood Scientific Ltd., Cambridge, U.K.). The data were corrected for diamagnetic susceptibilities.

The Cytotoxic Effect and Antiproliferative *in Vitro* Screening The synthesized Hoxa and its metal complexes were evaluated for their cytotoxic effects to rat peritoneal macrophages by MTT assay.

Further, the investigated compounds for antiproliferative effect to human colon and breast cancer cell lines, HCT-116 and MDA-231, respectively, by MTT assay were evaluated. The antiproliferative effect of these drugs was expressed as a percentage of inhibition of untreated cells proliferation. The HCT-116 and MDA-231 cells were mainted in Dulbecco's modified Eagle's medium supplemented with 10% fetal bovine serum. Cells were grown in culture bottles supplied with medium for cultivation, and after a few passages cells were seeded in 96-well plate. Cells were cultured in a humidified atmosphere of 5% CO_2 at 37°C during 24 h. The next 48 h the HCT-116 were incubated without and with 0.001, 0.01, 0.1, 1, 10 and 50 μM concentrations of the investigated compounds and MDA-231 cells were incubated without and with 0.01, 1 and 50 μM concentrations of the investigated compounds. Untreated HCT-116 and MDA-231 cells were cultivated only in medium for cultivation without investigated compounds and used as a control. After treatment with the investigated compounds during 48 h cell proliferation was determined by MTT assay. This test is based on the color reaction of mitochondrial dehydrogenase from living cells with MTT. Briefly, 10 μL of MTT solution (5 mg mL^{-1}) was added to each well after cells treatment during 48 h and cells incubate for an additional 3 h at 37°C. Produced formazan was dissolved by overnight incubation with sodium dodecyl sulfate (SDS)-HCl mixture (10% SDS in 0.01 N HCl) and absorbance was measured at dual wavelength of 570/650 nm with an enzyme-linked immunosorbent assay (ELISA) 96-well plate reader. The percentage of viable cells was calculated as the ratio between absorbance at each dose of the compounds and absorbance of untreated control cells ×100, and regarding the percentage of viable cells, the percent inhibition of cells proliferation was then calculated.

Characterization Oxaprozin (Hoxa): White solid, yield 72%, *Anal.* Calcd for $C_{18}H_{15}NO_3$ (%): C, 73.71; H, 5.15; N, 4.78. Found (%): C, 73.70; H, 5.36; N, 4.90. ^{1}H-NMR (DMSO-d_6): 12.36 (s, 1H, O–H), 7.30–7.59 (m, 10H, 2Ph-H), 3.06 (t, 2H, J=6.6 Hz, $CH_2\underline{CH_2}CO_2H$), 2.79 (t, 2H, J=7 Hz, $\underline{CH_2}CH_2CO_2H$); ^{13}C-NMR (DMSO-$d_6$): 173.5 (C1), 162.7 (C4), 144.9 (C5), 134.6 (C12), 132.3 (C13), 129.2 (C15, C17), 129.1 (C6), 128.9 (C8, C10), 128.7 (C16), 128.4 (C10), 127.7 (C14, C18), 126.6 (C7, C11), 30.5 (C2), 23.2 (C3). Selected FT-IR data (KBr) cm^{-1}: 3034 [ν(CH)], 2930 [ν(CH)], 2611 [ν(CH_2)], 1720 [ν(C=O)], 1568 [ν(CC)], 1502 [ν(CC)], 1443 [δ(CO), δ(CH_2)], 1362 [ω(CH), ν(CC)], 1275 [ω(CH_2), δ(COH)], 1060 [δ(CCC), ω(CH)], 965 [τ(HCCH)], 922 [γ(OHO)], 757 [δ(CH_2), γ(COC)], 586 [τ(CCOH), γ(O=COH)], 524 [γ(CC)].

[Mn(H_2O)$_2$(oxa)$_2$]·2H_2O (**1**): White solid, yield 62%, *Anal.*

Calcd for $C_{36}H_{36}MnN_2O_{10}$ (%): C, 60.76; H, 5.10; N, 3.94. Found (%): C, 60.53; H, 5.10; N, 3.97. Selected FT-IR data (KBr) cm^{-1}: 3294 [ν(OH)], 3058 [ν(CH)], 2943 [ν(CH)], 1566 [ν_{as}(COO)], 1549 [ν_{as}(COO)], 1447 [ν_s(COO)], 1431 [ν_s(COO)], 760 [$\delta(CH_2)$, γ(COC)], 696 [δ(CH), γ(CH)], 443 [ν(MnO)].

$[Co(H_2O)_2(oxa)_2]\cdot 2H_2O$ (**2**): Pink solid, yield 57%, *Anal.* Calcd for $C_{36}H_{36}CoN_2O_{10}$ (%): C, 60.42; H, 5.07; N, 3.92. Found (%): C, 60.32; H, 4.94; N, 3.94. Selected FT-IR data (KBr) cm^{-1}: 3381 [ν(OH)], 3277 [ν(OH)], 3031 [ν(CH)], 2949 [ν(CH)], 1568 [ν_{as}(COO)], 1549 [ν_{as}(COO)], 1502 [ν(CC)], 1446 [ν_s(COO)], 1414 [ν_s(COO)], 760 [$\delta(CH_2)$, γ(COC)], 696 [δ(CH), γ(CH)], 675 [δ(CCC)], 445 [ν(CoO)]. UV-Vis spectrum (nm): 478, 510, 560, 621.

$[Ni(H_2O)_2(oxa)_2]\cdot 2H_2O$ (**3**): Light blue solid, yield 79%, *Anal.* Calcd for $C_{36}H_{36}N_2NiO_{10}$ (%): C, 60.44; H, 5.07; N, 3.92. Found (%): C, 60.22; H, 5.06; N, 3.91. Selected FT-IR data (KBr) cm^{-1}: 3389 [ν(OH)], 3277 [ν(OH)], 3032 [ν(CH)], 2951 [ν(CH)], 1568 [ν_{as}(COO)], 1545 [ν_{as}(COO)], 1502 [ν(CC)], 1444 [ν_s(COO)], 1414 [ν_s(COO)], 760 [$\delta(CH_2)$, γ(COC)], 696 [δ(CH), γ(CH)], 675 [δ(CCC)], 447 [ν(NiO)]. UV-Vis spectrum (nm): 422, 714, 790.

$[Cu_2(H_2O)_2(OH)(oxa)_3]\cdot 2H_2O$ (**4**): Blue solid, yield 72%, *Anal.* Calcd for $C_{54}H_{51}Cu_2N_3O_4$ (%): C, 59.33; H, 4.70; N, 3.84. Found (%): C, 59.05; H, 5.00; N, 3.88. Selected FT-IR data (KBr) cm^{-1}: 3420 [ν(OH)], 3057 [ν(CH)], 2924 [ν(CH)], 1628 [ν_{as}(COO)], 1614 [ν_{as}(COO)], 1570 [ν(CC)], 1437 [ν_s(COO)], 764 [$\delta(CH_2)$, γ(COC)], 694 [δ(CH), γ(CH)], 443 [ν(CuO)]. UV-Vis spectrum (nm): 721.

$[Zn(H_2O)_2(oxa)_2]\cdot 1.5H_2O$ (**5**): White solid, yield 65%, *Anal.* Calcd for $C_{36}H_{35}N_2O_{9.5}Zn$ (%): C, 60.64; H, 4.95; N, 3.93. Found (%): C, 60.5; H, 4.92; N, 3.94. Selected FT-IR data (KBr) cm^{-1}: 3383 [ν(OH)], 3275 [ν(OH)], 3057 [ν(CH)], 2949 [ν(CH)], 1568 [ν_{as}(COO)], 1547 [ν_{as}(COO)], 1444 [ν_s(COO)], 1414 [ν_s(COO)], 762 [$\delta(CH_2)$, γ(COC)], 696 [δ(CH), γ(CH)], 445 [ν(ZnO)].

Results and Discussion

Synthesis, Characterization and Structural Formulae of the Complexes Oxaprozin was prepared according to the literature procedure[26] (Chart 1) and characterized by elemental analysis, ^{1}H-NMR, ^{13}C-NMR and FT-IR spectroscopy. All complexes were prepared by the ligand exchange reaction in aqueous solution (Chart 1) and characterized by elemental and TG analysis, FT-IR, UV-Vis spectroscopy and magnetic susceptibility measurements.

The formulae of the complexes **1**–**5** based on analytical and spectral data, TG analysis and assumption that coordination number of all TM ions is 6 are listed in Table 1. The complexes are referred to by the corresponding numbers in Table 1 hereinafter.

With the exception of **1**, which was dehydrated in a single step process, the results of TG analysis also allowed to distinguish between coordinated and uncoordinated H_2O molecules. Complexes **2**–**4** were dehydrated in two overlapped steps (Table 1) showing nearly equal mass loss in both steps. Complex **5** was dehydrated in two fairly separated steps: the first step up to 77.8°C can be attributed to the removal of $1.5H_2O$ molecules, whereas the remaining $2H_2O$ molecules were eliminated in the subsequent step up to 200.1°C. These observations, together with temperature ranges of dehydration and positions of differential thermalgravimetric (DTG) maxima (Table 1) show that the difference between binding energy of coordinated and uncoordinated H_2O molecules generally increases, while the overall energy required for total dehydration of the complexes approximately decreases in the order Co–Ni–Cu–Zn, *i.e.* both properties follow the order of TMs in the Periodic table. Again, the exception is the complex **1**.

FT-IR spectrum of Hoxa is in agreement with the literature.[27] In the spectra of **1**–**5** a new weak band that can be attributed to the M–O stretching vibrations appeared in the range 450–440 cm^{-1} and this band verifies oxa^- coordination as *O,O*-donor ligand.[23] ν(OH) stretching vibrations were found as very broad bands in the 3450–3250 cm^{-1} region confirming the presence of coordinated and uncoordinated water molecules. Except for **4**, FT-IR spectra of other complexes are almost identical indicating a great structural similarity.

The most prominent feature in the FT-IR spectra of **1**–**5** was the existence of two strong bands originating from the coordinated carboxylate groups [ν_{as}(COO) and ν_s(COO)] in the 1650 to 1420 cm^{-1} region (Table 1) . It is well-known that positions of these bands and their difference ($\Delta\nu$) are useful tool to predict the coordination mode of COO groups.[28,29] The $\Delta\nu$ values for the complexes (Table 1) were compared to the corresponding value ($\Delta\nu_i$=144 cm^{-1}) for purely ionic Naoxa salt, which was prepared by neutralization of Hoxa. The $\Delta\nu$ value of **4** is higher than that of Naoxa indicating monodentate or asymmetric bridging bidentate coordination mode of COO groups, whereas the $\Delta\nu$ values of **1**–**3** and **5** are lower than $\Delta\nu_i$ and correspond to the chelating coordination modes.

In the electronic spectrum of **2**, the highest energy transition $^4T_{1g}(F)\rightarrow{}^4T_{1g}(P)$, characteristic for distorted octahedral Co(II) complexes, was present at 478 nm. The band corresponding to the forbidden two-electron transition appeared as a shoulder at 621 nm. It was also possible to notice a spin-allowed transition assigned to $^4T_{1g}(F)\rightarrow{}^4A_{2g}(F)$ at 560 nm and one more spin forbidden transition at 510 nm originated in

Table 1. Structural Formulae, TG Data, Selected FT-IR Data and Magnetic Moments of the Complexes **1**–**5**

No.	Complex	TG analysis		ν_{as}(COO) (cm^{-1})	ν_s(COO) (cm^{-1})	$\Delta\nu$(COO) (cm^{-1})	μ_{eff} (BM)
		Total H_2O content, found (calcd) (%), and temperature range of dehydration (°C)	DTG maxima (°C)				
1	$[Mn(H_2O)_2(oxa)_2]\cdot 2H_2O$	9.7 (10.1), 30.0–140.6	103.9	1557	1431	126	5.82
2	$[Co(H_2O)_2(oxa)_2]\cdot 2H_2O$	9.4 (10.1), 45.1–193.4	107.2, 131.0	1557	1430	127	4.70
3	$[Ni(H_2O)_2(oxa)_2]\cdot 2H_2O$	10.2 (10.1), 33.3–158.6	72.8, 113.6	1556	1427	129	3.08
4	$[Cu_2(H_2O)_2(OH)(oxa)_3]\cdot 2H_2O$	6.6 (6.6), 25.0–118.1	64.8, 90.5	1621	1437	184	1.40
5	$[Zn(H_2O)_2(oxa)_2]\cdot 1.5H_2O$	8.3 (8.8), 29.9–200.1	56.8, 99.8	1556	1429	127	—

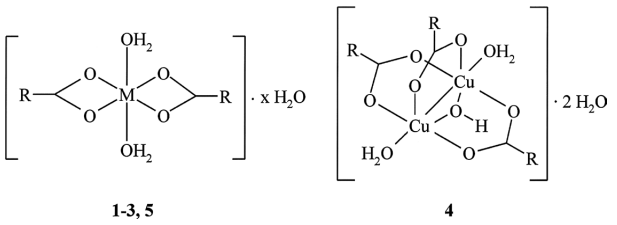

Fig. 1. Proposed Structures of the Complexes **1**–**5** (M=Mn, Co, Ni, Zn; x=2 for **1**–**3** and x=1.5 for **5**)

ROO represents an oxa^- ligand.

the ^2G state.[30] For **3**, three absorption bands: $^3A_{2g}\rightarrow{}^3T_{1g}(P)$, $^3A_{2g}\rightarrow{}^3T_{1g}(F)$ and $^3A_{2g}\rightarrow{}^3T_{2g}$ were observed at 422, 714 and 790 nm, respectively, also supporting distorted octahedral geometry.[30] In the electronic spectrum of **4**, a moderately strong, broad and asymmetric absorption band at 721 nm was found. The position of this band indicates the O_6 chromophore with D_2 or C_{2v} symmetry.[30] In general, the UV-Vis spectra of **2**–**4** are in accordance with (pseudo)octahedral geometry of the metal site.

The magnetic moment of **4** (1.40 BM) was considerably lower than spin-only value (1.73 BM[31]) demonstrating strong antiferromagnetic exchange interactions between the neighboring Cu(II) ions. A nearly identical value was also obtained by Dutta and co-workers for a very similar binuclear Cu(II) complex with formula $[Cu_2(DMSO)_2(oxa)_4]$ and very short Cu–Cu distance of 2.61 Å.[25] Therefore, an analogous dimeric formula (Table 1) and magnetic interactions are expected for **4**. Complexes **1**–**3** are high-spin and the corresponding μ_{eff} values (Table 1) are characteristic for (pseudo)octahedral coordination geometry of central TM ions.[31] In conclusion, colors, electronic spectra and magnetic moments unambiguously confirm octahedral or distorted octahedral coordination geometry of all complexes, as shown in Fig. 1.

Inhibition of Cancer Cell Proliferation The synthesized compounds were evaluated for inhibition of proliferation of human colon and breast cancer cell lines, HCT-116 and MDA-231, respectively. The cell proliferation was determined by MTT assay after 48 h of treatment with Hoxa and **1**–**5** in the 0.001–50 μM range of concentration.

Investigation of antiproliferative activities of Hoxa and **4** on HCT-116 cell line (Table 2) showed an increased activity with increased concentration. Thus, Hoxa in the 0.1, 1 and 10 μM concentration and **4** in the 1, 10 and 50 μM have statistically significant inhibitory potency. The inhibitory potency of **5** to HCT-116 cells proliferation is significant only in 0.1 and 50 μM. On the contrary, complexes **1**–**3** showed excellent inhibition of HCT-116 cells proliferation in the whole concentration range. The best values of percentage of inhibition were expressed by **3** (Fig. 2). These results indicate a very potent antiproliferative potency of **3** in the lowest concentration (0.001 μM) and it will be the base for future studies.

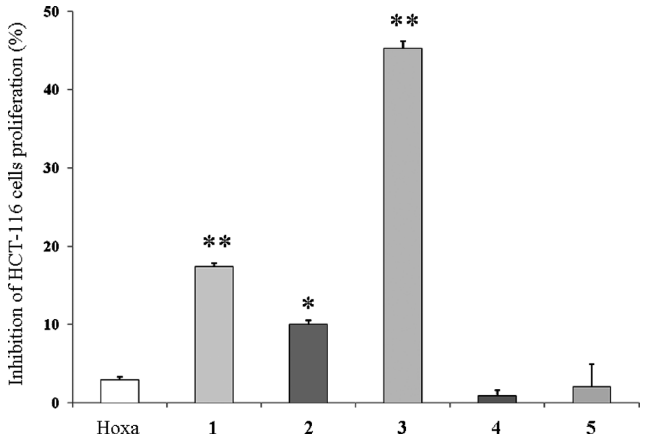

Fig. 2. The Antiproliferative Effect of Hoxa and **1**–**5** on HCT-116 Cell Line at Concentration of 0.001 μM

*p<0.05; **p<0.01 *vs.* nontreated cells.

The results of inhibitory activity of Hoxa and **1**–**5** on the other tumor cell line, MDA-231 are also shown in Table 2. It is evident that **2** and **5** in the highest investigated concentration and **5** in the lowest concentration exhibit inhibitory effect on MDA-231 cells proliferation. Hoxa, as well as **1**, **3** and **4** demonstrated statistically significant potent capacity of inhibition of MDA-231 cells proliferation in all investigated concentrations.

Presented results of antiproliferative activity of the investigated complexes at lower concentrations are in agreement with the literature data[23–25] about increased biological activities of TM complexes of NSAIDs in comparison to the activity of their parent drugs. Especially, an improved antiproliferative activity of **1** and **3** against HCT-116, as well as of **1**, **3** and

Table 2. The Antiproliferative Effect of Hoxa and **1**–**5** on HCT-116 and MDA-231 Cell Lines

Concentration (μM)	Inhibition of HCT-116 cells proliferation (%)					
	Hoxa	**1**	**2**	**3**	**4**	**5**
0.001	2.9±0.4	17.4±0.4**	10.0±0.5*	45.3±0.9**	0.9±0.7	2.0±2.9
0.01	1.0±1.2	12.7±0.8**	13.5±0.7*	7.1±0.5*	1.3±1.4	1.1±2.25
0.1	15.5±0.9*	13.7±0.3**	8.9±0.4*	19.5±0.2**	2.6±1.1	14.4±0.68*
1	32.1±0.7**	12.8±0.6*	9.6±0.4*	14.6±0.3**	9.4±0.3*	0.8±1.4
10	52.7±0.8**	17.2±0.3**	9.9±0.4*	27.8±1.1*	15.1±0.6*	0.9±0.4
50	—[a]	2.9±0.4	18.6±0.9*	38.1±0.7**	25.4±0.4**	18.6±0.4**
	Inhibition of MDA-231 cells proliferation (%)					
0.01	15.7±0.5**	22.8±0.2**	4.5±0.8	17.8±0.2*	19.9±0.1**	16.5±0.5*
1	42.9±0.4**	26.7±0.6*	12.1±0.5	19.2±0.2*	19.6±0.4*	13.1±0.4
50	—[a]	65.6±0.2**	61.4±0.1***	60.5±0.2**	52.8±0.3***	41.8±0.2***

*p<0.05; **p<0.01; ***p<0.001 *vs.* nontreated cells. *a*) This concentration can not be measured due to limited solubility of Hoxa in the medium for cell cultivation.

4 against MDA-231 cancer cell lines has shown (Table 2).

Dose-dependent antiproliferative effects to HCT-116 cell line were observed for Hoxa and **4**. However, dose-dependent effects were not found for **1**–**3**, but these compounds showed good antiproliferative activity in all investigated concentrations (excluding **1** in the highest concentration). Such unexpected antiproliferative activity of **1**–**3** can be explained with different type of induced cell death (apoptosis and necrosis) of treated cells and various mechanisms of apoptosis.[6–8] Further, with exception of **2** and **5**, dose-dependent antiproliferative effects to MDA-231 cell line for other investigated compounds were also found.

The complex **5** showed inhibitory potency to HCT-116 cells only at the concentrations of 0.1 and 50 μM, and to MDA-231 cells only at the concentrations of 0.01 and 50 μM. A plausible explanation for diverse inhibitory potency of **5** in comparison to other compounds could be different modes of action of **5** at low and high concentration. It could be assumed that in low concentration **5** has a similar satisfactory effect as all other investigated compounds. However, at high concentrations release of high amounts of Zn(II) ions in culture medium could induce rapid uptake of these ions by the cells and promote a caspase-independent alternative apoptosis pathway.[32]

For confirmation of antiproliferative effects of Hoxa and **1**–**5** an additional examination of cytotoxic effect (non-specific cells killing) to viability of unstimulated and lipopolysaharide (LPS) stimulated rat peritoneal macrophages by MTT assay was conducted. This part of the study demonstrated that Hoxa and **1**–**5** did not exhibit the cytotoxic effect to peritoneal macrophage (data not shown), which is well-known cell used for this type of investigation.

Conclusion

Oxaprozin and its complexes with Mn(II), Co(II), Ni(II), Cu(II) and Zn(II) were synthesized and characterized. A distorted octahedral geometry was proposed for all complexes. All complexes exhibited significant antiproliferative activity against human colon and breast cancer cell lines, HCT-116 and MDA-231, respectively. Especially, Ni complex showed very potent antiproliferative effect on HCT-116 cell line at concentration of 0.001 μM with inhibition of 45.3±0.9%.

Acknowledgements The authors acknowledge the financial support of the Ministry of Education and Science of the Republic of Serbia (Grants No. 172013 and III45007).

References

1) al-Faks M. A., Pugh M. C., *Orthop. Rev.*, **21**, 558–560, 560–563 (1992).
2) Talley J. J., Brown D. L., Carter J. S., Graneto M. J., Koboldt C. M., Masferrer J. L., Perkins W. E., Rogers R. S., Shaffer A. F., Zhang Y. Y., Zweifel B. S., Seibert K., *J. Med. Chem.*, **43**, 775–777 (2000).
3) Baron J. A., *Prog. Exp. Tumor Res.*, **37**, 1–24 (2003).
4) Ettarh R., Cullen A., Calamai A., *Pharmaceuticals* (Ott.), **3**, 2007–2021 (2010).
5) Bottone F. G. Jr., Moon Y., Kim J. S., Alston-Mills B., Ishibashi M., Eling T. E., *Mol. Cancer Ther.*, **4**, 693–703 (2005).
6) Basu G. D., Pathangey L. B., Tinder T. L., Lagioia M., Gendler S. J., Mukherjee P., *Mol. Cancer Res.*, **2**, 632–642 (2004).
7) Sun Y., Sinicrope F. A., *Mol. Cancer Ther.*, **4**, 51–59 (2005).
8) Tegeder I., Pfeilschifter J., Geisslinger G., *FASEB J.*, **15**, 2057–2072 (2001).
9) Ou Y. C., Yang C. R., Cheng C. L., Raung S. L., Hung Y. Y., Chen C. J., *Eur. J. Pharmacol.*, **563**, 49–60 (2007).
10) Yip-Schneider M. T., Schmidt C. M., *Pancreas*, **27**, 337–344 (2003).
11) Rice P. L., Goldberg R. J., Ray E. C., Driggers L. J., Ahnen D. J., *Cancer Res.*, **61**, 1541–1547 (2001).
12) Rice P. L., Beard K. S., Driggers L. J., Ahnen D. J., *Cancer Res.*, **64**, 8148–8151 (2004).
13) Liou J. Y., Ghelani D., Yeh S., Wu K. K., *Cancer Res.*, **67**, 3185–3191 (2007).
14) Baek S. J., Kim J. S., Moore S. M., Lee S. H., Martinez J., Eling T. E., *Mol. Pharmacol.*, **67**, 356–364 (2005).
15) Wahl C., Liptay S., Adler G., Schmid R. M., *J. Clin. Invest.*, **101**, 1163–1174 (1998).
16) Ho C. C., Yang X. W., Lee T. L., Liao P. H., Yang S. H., Tsai C. H., Chou M. Y., *Eur. J. Clin. Invest.*, **33**, 875–882 (2003).
17) Iizuka Y., Sakurai E., Tanaka Y., *Riken Review*, **35**, 3–4 (2001).
18) Lippard S. J., Berg J. M., "Principles of Bioinorganic Chemistry," University Science Books, Mill Valley, 1994, p. 411.
19) Szilagyi R. K., Bryngelson P. A., Maroney M. J., Hedman B., Hodgson K. O., Solomon E. I., *J. Am. Chem. Soc.*, **126**, 3018–3019 (2004).
20) Stipanuk M. H., "Biochemical, Physiological & Molecular Aspects of Human Nutrition," 2nd ed., W. B. Saunders Company, New York, 2006, pp. 1043–1067.
21) Kobayashi M., Shimizu S., *Eur. J. Biochem.*, **261**, 1–9 (1999).
22) Lay P., Hambley T., WO Patent 109843 (2007).
23) Sadaf Y., Saqib A., Bushra M., Fiaz A., Saira S., *J. Coord. Chem.*, **62**, 3463–3470 (2009).
24) Saha D. K., Padhye S., Padhye S., *Met. Based Drugs*, **8**, 73–77 (2001).
25) Dutta S., Padhye S., Mckee V., *Inorg. Chem. Commun.*, **7**, 1071–1074 (2004).
26) Brown K., US Patent 3578671 (1971).
27) Sagdinc S. G., Esme A., *Spectrochim. Acta [A]*, **75**, 1370–1376 (2010).
28) Deacon G. B., Phillips R., *Coord. Chem. Rev.*, **33**, 227–250 (1980).
29) Nakamoto K., "Infrared and Raman Spectra of Inorganic and Coordination Compounds, Part B, Applications in Coordination, Organometallic and Bioinorganic Chemistry," 5th ed., John Wiley & Sons, New York, 1997, pp. 59–62.
30) Lever B. P., "Inorganic Electronic Spectroscopy," 2nd ed., Elsevier, Amsterdam, 1984, pp. 480–505, 507–544, 554–568.
31) Greenwood N. N., Earnshaw A., "Chemistry of the Elements," 2nd ed., Elsevier, Oxford, 1998, pp. 1060, 1132, 1158, 1193.
32) Buerki-Thurnherr T., Xiao L., Diener L., Arslan O., Hirsch C., Maeder-Althaus X., Grieder K., Wampfler B., Mathur S., Wick P., Krug H., *Nanotoxicology* (2012). doi:10.3109/17435390.2012.666575